3rd IAA Conference on Space Situational Awareness (ICSSA)

Madrid, Spain

IAA-ICSSA-22-00-00
CENTROIDING TECHNIQUE USING MACHINE LEARNING ALGORITHM FOR SPACE OPTICAL NAVIGATION

Aurelio Kaluthantrige[1], **Jinglang Feng**[2], **Jesús Gil-Fernández**[3], **Andrea Pellacani**[4]

[1] *University of Strathclyde, James Weir Building 75 Montrose St, G1 1XJ, Glasgow, United Kingdom, +44 07862678235, Mewantha.kaluthantrige-don@strath.ac.uk*

[2] *University of Strathclyde, James Weir Building 75 Montrose St, G1 1XJ, Glasgow, United Kingdom, +44 01415482473, jinglang.feng@strath.ac.uk*

[3] *ESA/ESTEC, Keplerlaan 1, 2200 AG Noordwijk, The Netherlands, Jesus.Gil.Fernandez@esa.int*

[4] *GMV Aerospace and Defence, Isaac Newton 11 PTM, 28760 Tres Cantos, Madrid, Spain, apellacani@gmv.com*

Keywords: *Asteroid deflection, Optical Navigation, Image Processing, Centroiding Technique, Machine Learning.*

ABSTRACT

Near-Earth-Objects pose a major threat to our planet with potential impacts. Together with the National Aeronautics and Space Administration (NASA), the European Space Agency (ESA) launched the Asteroid Impact Deflection Assessment (AIDA) international collaboration to demonstrate the deflection of the trajectory of binary asteroid system (65803) Didymos with kinetic impact. ESA's HERA mission will arrive at Didymos in 2026 to observe closely NASA's DART impact effects . This paper focuses on the Early Characterization Phase (ECP) and the Detailed Characterization Phase (DCP) of the proximity operations of HERA. The objective of these phases is to achieve physical and dynamical characterizations of Didymos. The optical navigation is applied to determine the relative state of the spacecraft with respect to the asteroid by detecting its Centre of Mass (COM). This can be achieved by the centroiding technique with the images captured by the spacecraft on-board camera and the Image Processing (IP) algorithm.

Nevertheless, the standard IP algorithms depend thoroughly on the visibility of the target in the images, and they lack of robustness in case of adverse illumination conditions or if the target is partially out of the camera frame. To address these insufficiencies, this paper develops a model of IP based on the High-Resolution Network (HRNet) Machine Learning algorithm. With its convolutional layers, the HRNet is capable of extracting specific information from images without dependency on the quality of the image itself. Furthermore, the HRNet is capable of preserving the high-resolution of the image with superior spatial precision, which is desirable for estimating specific features such as the center of an asteroid. The training, validation and testing datasets

are generated using the software Planet and Asteroid Natural scene Generation Utility (PANGU). The performances of the HRNet-based IP algorithm are evaluated in terms of Root Mean Squared Error (RMSE) between the pixel coordinates of the estimated and the true centroid of Didymos. The results shows that the HRNet-based IP algorithm is capable of regressing the position of the centroid with high accuracy and without being affected by the illumination conditions or if the asteroid is partially out of the camera frame.

1. Introduction

Small bodies (below $10\ m$ in size) collide with Earth without leading to any severe consequences while more than 90% of larger bodies ($1\ km$ or more in size) poses no risk of collision. On the other hand, intermediate size (100-$500\ m$ in size) bodies collisions can happen more frequently and can procure regional scale damages. Therefore, space agencies put in place strategic means to prevent intermediate size asteroids impact. For this to happen it is necessary to improve the knowledge of the physical and dynamical properties of these bodies and test methods to deflect them.
AIDA is an international collaboration that aims to demonstrate asteroid impact hazard mitigation using a kinetic impactor [1]. The latter is the Double Asteroid Redirection Test (DART), developed by NASA and launched on the 24th of November 2021. ESA's contribution to AIDA is HERA, an asteroid exploration mission that will be launched in October 2024. The objectives of HERA are to determine the momentum transfer by the impact of DART, to carry a physical and dynamical characterization of the asteroid and to perform close-proximity operations [2].
The target body of AIDA is the binary asteroid system (65803) Didymos, which consists of the primary body and its moon, Dimorphos. Table 1 reports relevant properties of the binary asteroid system. The spin axes of the primary and the secondary and the angular momentum of the secondary's orbit around the primary are all parallel. Dimorphos' rotation period is equal to its revolution period around the primary [3].

Table 1: Didymos' system properties [3]

Parameter	Didymos	Dimorphos
Gravitational parameter [km^3/s^2]	$3.5225 \cdot 10^{-8}$	$2 \cdot 10^{-10}$
Diameter [m]	780	164
Rotation period [$hours$]	2.26	11.92
Obliquity of the binary orbit with Ecliptic plane	$169.2°$	$169.2°$

The proximity operations are divided in different phases depending on the mission objectives. The first phase is the Early Characterization Phase, and it starts after the execution of the capture manoeuvre around Didymos. The objective is to characterize the size, shape and main dynamical properties of both bodies by imaging. The only navigation instrument is the Asteroid Framing Camera (AFC) and it is desired that both bodies lie within its Field Of View (FOV). The spacecraft is kept at a distance of around $30\ km$ from the target. The ECP is followed by the Payload Deployment Phase (PDP) when the release of the CubeSat carried on board occurs. The next phase

is the Detailed Characterization Phase, which has the objective of characterizing Dimorphos' mass and density at a distance of around $10\ km$ from the target. The AFC is still the only navigation instrument employed and the trajectory is designed so that the image of the primary is always fully within the FOV. The DCP is followed by the Close Observation Phase (COP), which has the primary objective of characterizing DART's impact. Therefore, the distance from the binary system is reduced to $4\ km$ approximately, in order to capture high resolution images of the secondary. The last phase is the Experimental Phase (EXP), which has a lower distance from the surface of Didymos with respect to the COP, in order to obtain very high-resolution images of the crater generated by DART's impact. Because of the lower distances, Didymos will not fit entirely in the FOV during the COP and the EXP, hence the AFC camera is juxtaposed with the Planetary ALTimeter (PALT) to improve navigation performances.
Observing a binary asteroid system from such a short distance requires a high level of autonomy for the Guidance Navigation and Control (GNC) system, which is achieved with a vision based navigation system. The latter relies on an IP algorithm that extracts visual data from the images taken from the AFC camera [4].
For the ECP and the DCP the navigation strategy is based on estimating the centroid of the asteroid, i.e. its Center of Mass, to enable autonomous attitude navigation [5]. Nevertheless, standard IP algorithms' performances are highly depending on the intrinsic properties of the captured images. Factors such as the Signal-to-Noise ratio, illumination conditions and the presence of other bodies in the image can affect the accuracy of the extracted visual information. Moreover, standard IP algorithms rely on the shape of the asteroid; therefore, the performance of these algorithms can be damaged if the target body is partially outside of the FOV.
Methods that estimate the COM of the asteroid applying an offset to the Center of Brightness (COB), the centroid of the image when each pixel is weighted by its intensity, have been proposed. The offset depends on the position of the Sun, therefore the performances of these algorithms are highly depending on the lighting conditions [6]. Data-driven scattering laws have been implemented to solve the dependency of the accuracy of these methods on the position of the Sun [7].
Centroid Apparent Diameter (CAD), ellipse and limb fitting techniques rely on the a priori knowledge of the apparent size and shape of the asteroid. Hence their accuracy can be damaged if the asteroid is partially outside of the FOV [8, 9].
The current IP algorithm implemented by HERA for the centroiding problem resolution is the Maximum Correlation with a Lambertian Sphere (MCLS). This algorithm estimates the size of the sphere with Lambertian reflectance that maximises the normalized correlation with the binarized image of the asteroid. Hence, the bright pixels of the image and the visible shape of the asteroid affect the performances of this IP algorithm [5].
In this work, we develop a Convolutional Neural Network (CNN)-based image processing algorithm that estimates the centroid of Didymos without being affected by its illumination condition and in the event its shape is partially outside of the image. The algorithm is applied to the ECP and the DCP phases of the proximity operations of HERA.
The main advantages of CNNs with respect to standard IP algorithm is the independency of the performance from the adverse characteristics of the images [10]. This can improve the navigation performances and allow reducing the complexity on the navigation filter. Most of the CNNs process the input image with a network typically

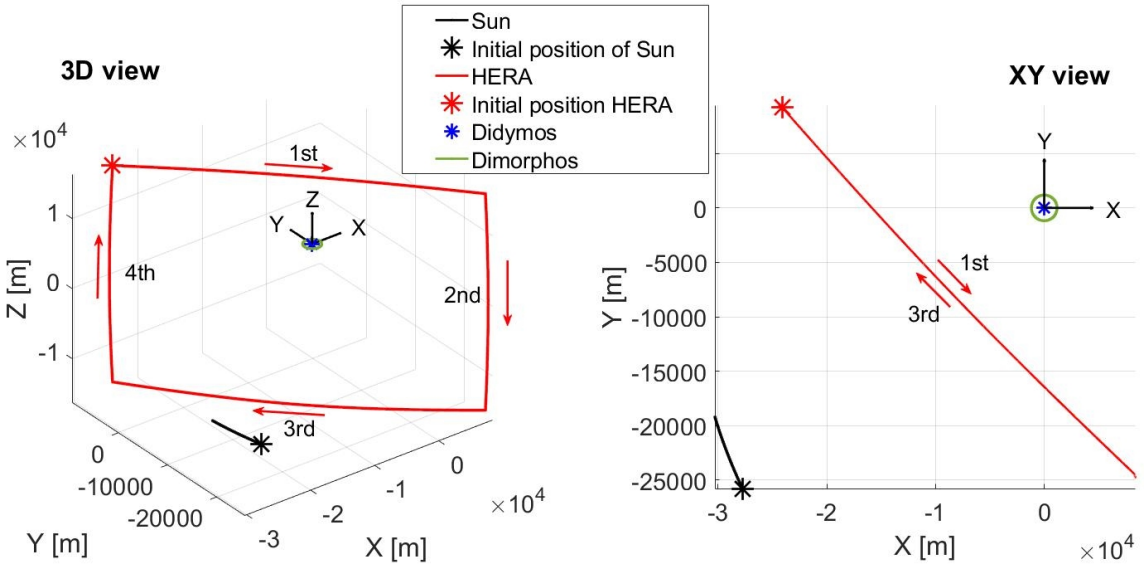

Figure 1: ECP trajectory

consisting of a series of high-to-low resolution subnetworks. This process reduces the input's resolution, which is then recovered through a low-to-high process. With this procedure, extracted visual data have low spatial precision and accuracy that are important requirements of an autonomous navigation system. Therefore, this work adopts the High-Resolution Network CNN architecture to maintain a high-resolution representation through the whole network [11]. This process leads to a features extraction with superior spatial precision and higher accuracy.
For the application to the HERA mission, the HRNet-based IP algorithm is capable to estimate with high accuracy the centroid of Didymos, and its performances are not affected by the illumination conditions or in the event that the target body does not lie entirely within the FOV.
This paper is structured as follows. Section 2 illustrates the reference trajectories of this work. Next, Section 3 describes the framework of our methodology. Section 4 performs the numerical simulations and analyze the results obtained. Finally Section 5 concludes this research and recommends future research directions.

2. Reference trajectory

In this Section, the ECP and DCP trajectories of HERA employed in this work are described. The adopted reference frame is the Target Body Equatorial Inertial (TBEqI), which has the origin located on Didymos, the X-axis pointing towards the vernal equinox, and the XY plane coplanar to the equatorial plane of Didymos. The relative motion of the Sun around Didymos is retrograde as the binary system's orbit obliquity with respect to the Ecliptic plane is higher than 90 degrees, as shown in Table 1.

2.1. Early Characterization Phase

The ECP trajectory data is provided by ESA. Figure 1 represents the trajectory of the spacecraft, together with the position of the Sun (scaled down in the illustration) and the orbit of the secondary. The position of the Sun is calculated using the Jet

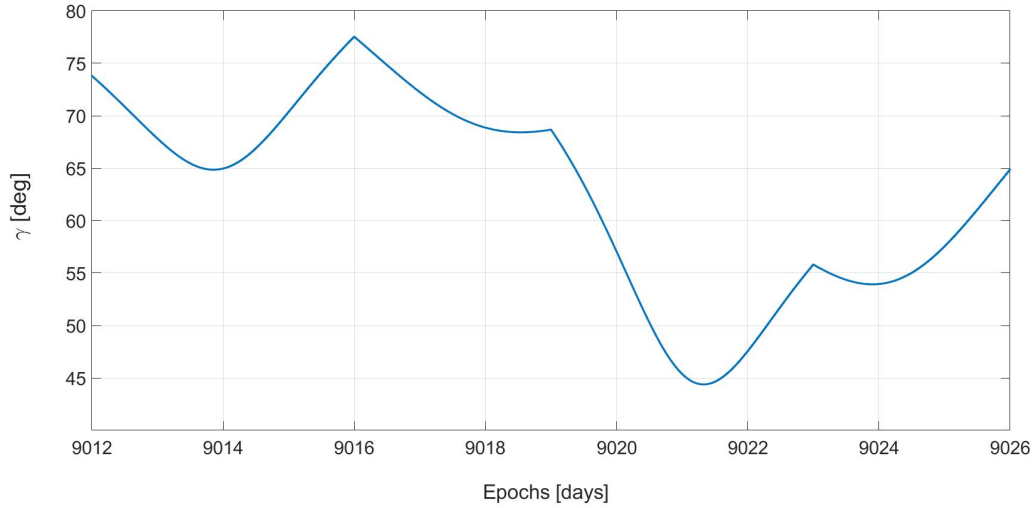

Figure 2: Phase angle ECP

Propulsion Laboratory Small Body Database [12].
The trajectory consists of 4 hyperbolic arcs, with an initial epoch of $t_{in} = 9012$ days and a final epoch of $t_{fin} = 9026$ days, calculated in the Modified Julian Date 2000. The only forces considered for each arc are the point mass gravitational attractions of both the primary and the secondary. Orbital manoeuvres are performed at the joint of two arcs. The duration of the 1^{st} and 3^{rd} arcs is 4 days while the duration of the 2^{nd} and 4^{th} arcs is 3 days. The range with respect to the primary varies between a minimum of $20\ km$ and a maximum of $30\ km$. It can be seen from Figure 1 that the ECP trajectory is interposed between the Sun and Didymos, in order to provide the AFC camera with bright images for the centroiding navigation [4]. Figure 2 shows that the phase angle γ (Sun-asteroid-HERA angle) for the ECP trajectory is lower than 90 degrees, meaning that HERA is always seeing the day side of the asteroid.

2.2. Detailed Characterization Phase

The DCP trajectory data is provided by GMV Aerospace and Defence. Figure 3 represents the trajectory of the spacecraft, together with the position of the Sun (scaled down in the illustration) and the orbit of the secondary.
The trajectory consists of 8 hyperbolic arcs with a total duration of 28 days. The first arc is the transition between ECP and DCP, followed by repetitive trajectories with a range with respect to the primary varying between approximately $9\ km$ and $23\ km$, as shown in Figure 4. The minimum distance of $9\ km$ is designed to ensure that the full shape of Didymos is within the FOV even in the presence of $100\ m$ navigation error [4].

3. Methodology

In this Section, the methodology of this research is described. The process to generate images from the reference trajectories is illustrated followed by the implementation of the HRNet-based centroiding algorithm.

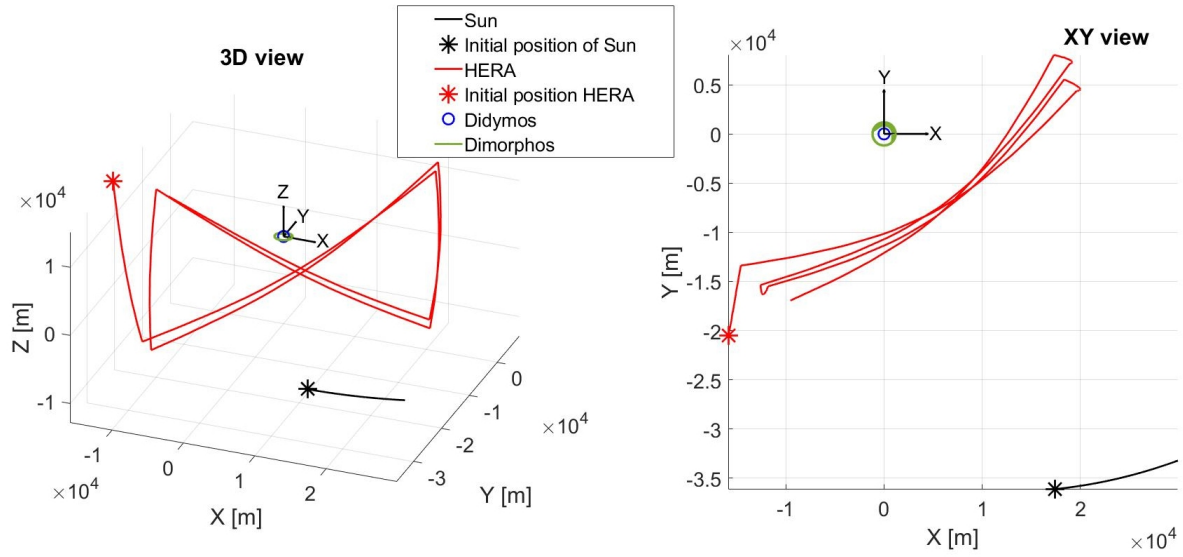

Figure 3: DCP trajectory

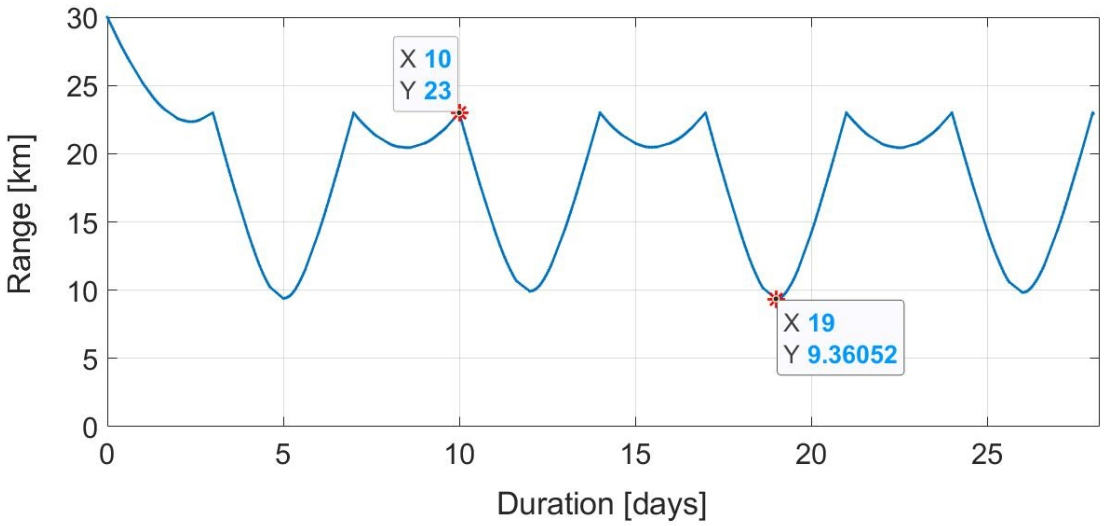

Figure 4: Range of DCP

3.1. Generation of images

The software Planet and Asteroid Generation Utility is used to generate the database of images for the training, validation and testing of the HRNet. PANGU is a simulation tool that models planet and asteroids surfaces and provides a high degree of realism in the visualization of images while operating at near real-time speeds. The software has been developed by the STAR-Dundee engineering company [13].

The models of Didymos, Dimorphos and the camera are provided by GMV Aerospace and Defence. Didymos' shape is a spinning top with an elevated ridge along the equator, giving it a quasi-spherical shape, while the shape of Dimorphos is not well known except that it appears to be ellipsoidal. The model of Itokawa, the target asteroid of the Hayabusa mission, is scaled down and used to simulate Dimorphos. The pinhole camera model is implemented in the software using the properties of the AFC camera,

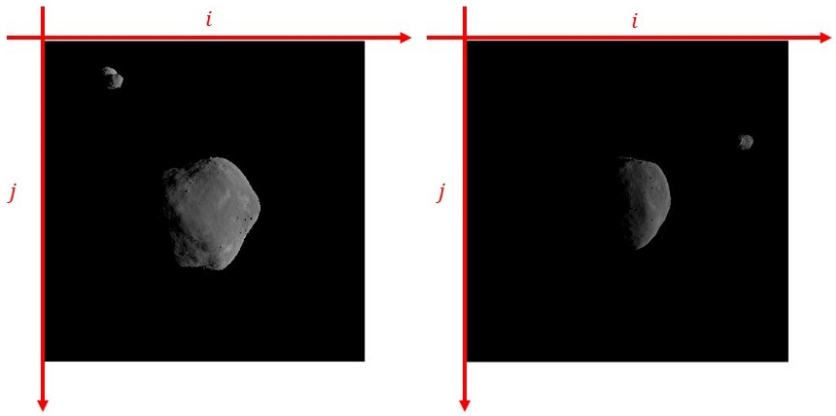

Figure 5: PANGU viewer with two sample images captured at different points of the ECP trajectory

shown in Table 2 [14].

Table 2: AFC properties [14]

FOV	Focal Length	Aperture	Image size
5.5°	10.6 cm	2.5 cm	1024×1024 $pixels$

The software generates the images detected by the camera and shows them on the PANGU viewer, a plane with the size of the image (shown in Table 2) and the origin set to the top left corner. The horizontal and the vertical axes of the plane are referred to as i-direction and j-direction respectively.
In order to visualize the binary system of asteroids on PANGU, the flight file system is operated. These files control the PANGU viewer and generate images taken at each point of the reference trajectories, considering, in the TBEqI reference system, the position of the Sun (range, Azimuth and Elevation) and the positions and the orientations (quaternions) of the binary asteroid system and the AFC camera (joined with HERA) [13].
During asteroid imaging, the AFC has its boresight pointing towards the asteroid and the vertical axis of the camera is perpendicular to the direction of the Sun with respect to the spacecraft [4]. PANGU takes the boresight, the vertical and the horizontal axis of the camera respectively as the Z- the Y- and the X-axis of the camera reference frame [13]. Therefore, the position vector of the Sun with respect to HERA lies on the XZ plane of the camera frame. As a result, the images generated on the PANGU viewer always represent the binary system illuminated from the right side. Figure 5 shows two sample images generated at different points of the ECP trajectories, together with the i- and the j-directions of the PANGU viewer.
When the camera is pointing perfectly towards the primary, the latter is displayed at the middle of the PANGU viewer. The implemented models of Didymos and Dimorphos in PANGU, in these conditions, have the central pixel, with coordinates $(i, j) = (512, 512)$ pixels, representing the Geometrical Center (GC) of the target body, that is the arithmetic mean position of all the points belonging to the body. Because of its quasi-spherical shape, the COM of the primary almost coincides with its GC. Since the im-

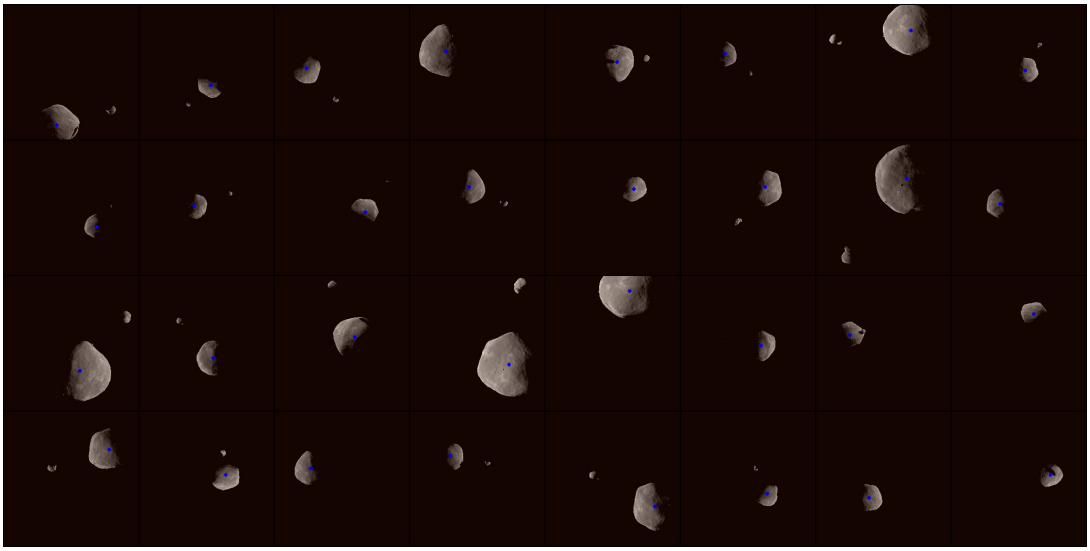

Figure 6: Sample keypoints detection results during training

ages used in this work are all generated with PANGU, it is assumed that the GC of Didymos is its centroid.
If the camera's boresight is always pointing perfectly towards the GC of the asteroid, its position on the PANGU viewer will always be $(i, j) = (512, 512)$ pixels for each image. Training the CNN algorithm with a set of image with these characteristics will result in an issue of label variability. To overcome this issue a pointing error represented by spherical coordinates and defined by two angles α and β is introduced at each point of the trajectory, so that the generated images are shifted from their central position of the PANGU viewer.
In order to generate a dataset of images always representing the asteroid within the FOV, random values within an interval of $[-1.9, 1.9]$ degrees are considered for α and β. With these values, the primary location is shifted around the viewer, sometimes partially outside of the frame. By calculating the shift in pixels of the primary from its central position, the pixel coordinates of the GC of the primary is calculated for each value of α and β.

3.2. HRNet

The HRNet is the state-of-the-art technology in detecting visual data (keypoint) from images, with its capabilities of maintaining high-resolution representations of the input images by connecting multiple subnetworks in parallel. Each layer of the architecture is formed from the gradual addition of previous stages high-resolution subnetworks with repeated multiscale fusions. The last high-resolution representation is then used for the regression of the desired keypoint, in this work being the centroid of Didymos.
The input database for the ECP consists of 12104 (60.16%) images for training, 1513 (7.52%) images for validation and 6052 (30.08%) images for testing obtained by sampling the trajectory respectively every 100, 800 and 200 seconds. The images generated with the DCP are 450 (2.24%), i.e. sampling every hour the trajectory, and are used for the testing dataset.
Each input image of the HRNet is coupled with the corresponding centroid of Didymos,

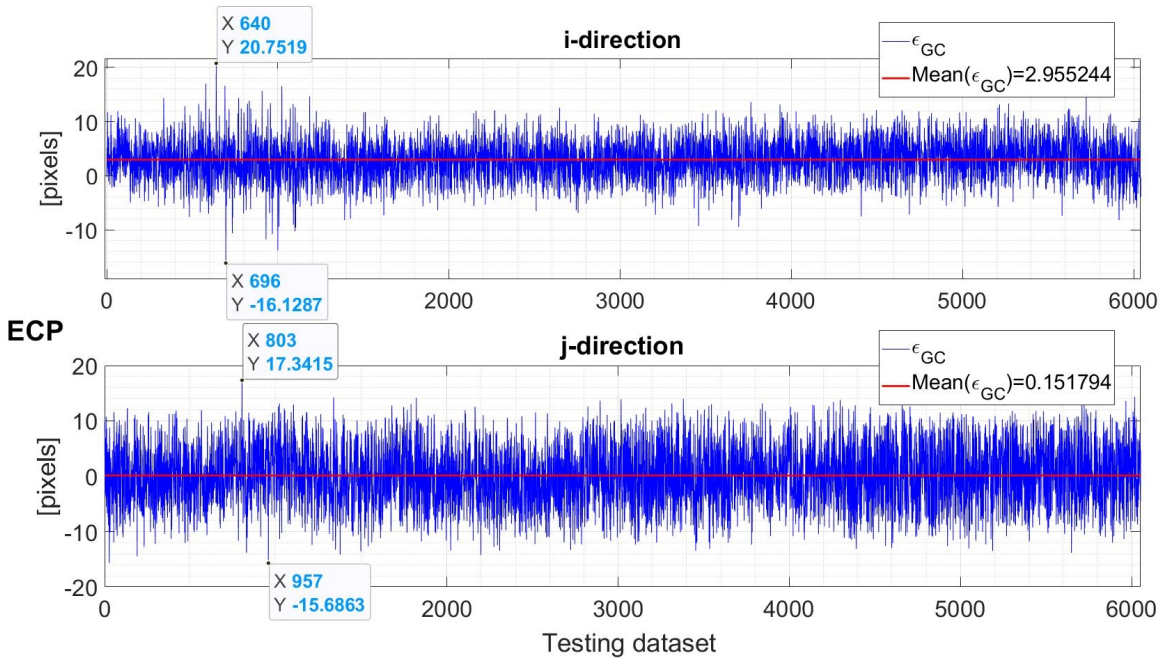

Figure 7: ε_{GC} for ECP

which represents the Ground Truth (GT) keypoint, used to supervise the training and validation of the HRNet. In this work, the pose-hrnet-w32 is used, where 32 represent the widths of the high-resolution subnetwork in the last three stages. The Adam optimizer is used with a cosine decaying learning rate with initial value of 10^{-3} and decaying factor of 0.1. The total parameters involved in the training are $28,535,585$. The network is trained for 210 epochs. Figure 6 shows a mosaic of keypoint detection results on a subset of the training dataset.

4. Results

In this section, the results of the HRNet-based IP algorithm for the centroid estimation of Didymos are presented. Firstly, the results on the testing database of the ECP are shown by examining the accuracy of the algorithm and the influence of the Sun phase angle. Secondly, the case of Didymos located partially out of frame is analyzed. Finally, the results on the testing database of the DCP are shown. The metrics to evaluate the performances are defined as follows:

$$\varepsilon_{GC} = GC_{GT} - GC_{pred} \tag{1}$$

$$RMSE = \sqrt{\frac{\sum_{i=1}^{N}(GC_{GT}^{i} - GC_{pred}^{i})^2}{N}} \tag{2}$$

where ε_{GC} represents the error in pixels between the ground truth GC and the estimated GC, and $RMSE$ is the Root Mean Squared Error in pixels between the same quantities. Both metrics are evaluated for each direction of the PANGU viewer.
To evaluate the accuracy of the developed algorithm, the $RMSE$ values for the i- and j-directions obtained by the MCLS IP algorithm developed by GMV Aerospace and Defence for the HERA mission are given as a reference: $RMSE_i^{GMV} = 5.987$ pixels and

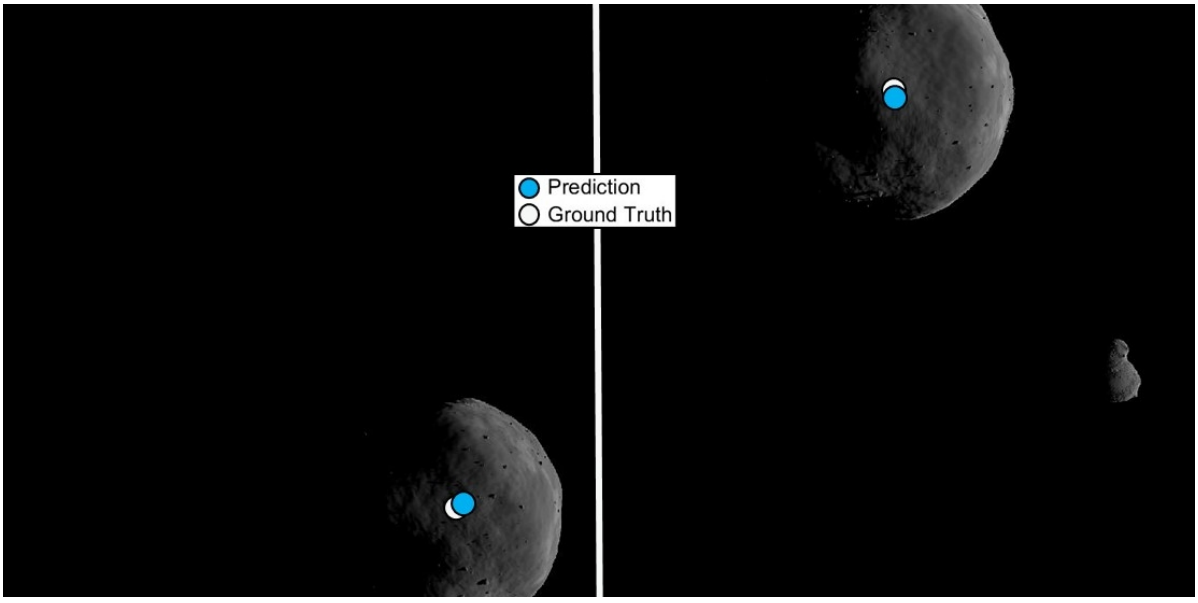

Figure 8: Centroiding results for images representing Didymos partially out of frame

$RMSE_j^{GMV} = 4.915$ pixels. These results are obtained by applying the algorithm over a set of 243 images generated during the ECP.

4.1. ECP

4.1.1. Accuracy

Figure 7 represents the ε_{GC} for the centroiding of Didymos for both i and j-directions of the PANGU viewer reference frame, for the testing dataset of 6052 images of the ECP. It can be seen that the error is oscillating around 2.95 pixels in the i-direction with a maximum and a minimum values of 20.75 and -16.12 pixels and around 0.15 pixels in the j-direction with a maximum and a minimum values of 17.34 and -15.68 pixels, respectively. The $RMSE$ values are: $RMSE_i = 4.77$ pixels and $RMSE_j = 5.65$ pixels, which are similar to the ones obtained by the MCLS IP algorithm. Therefore, the HRNet-based IP algorithm is able to estimate the centroid of the primary with high accuracy.

4.1.2. Phase Angle

As mentioned in Section 3.1, the binary asteroid system is always illuminated from the right side in the images. Hence, the influence of the Sun phase angle can be inferred by the results on the i-direction. The systematic error of 2.95 pixels is negligible considering that is lower than the peak-to-peak amplitude (36.87 pixels) of the error itself. Therefore, the developed centroiding algorithm is not affected by the illumination conditions of the asteroid.

4.2. Didymos partially out of frame

The subset of images that represents Didymos partially outside of the camera frame consists of 279 out of the 6052 images of the testing dataset. The RMSE values of the developed centroiding algorithm for these images are: $RMSE_i = 5.78$ pixels

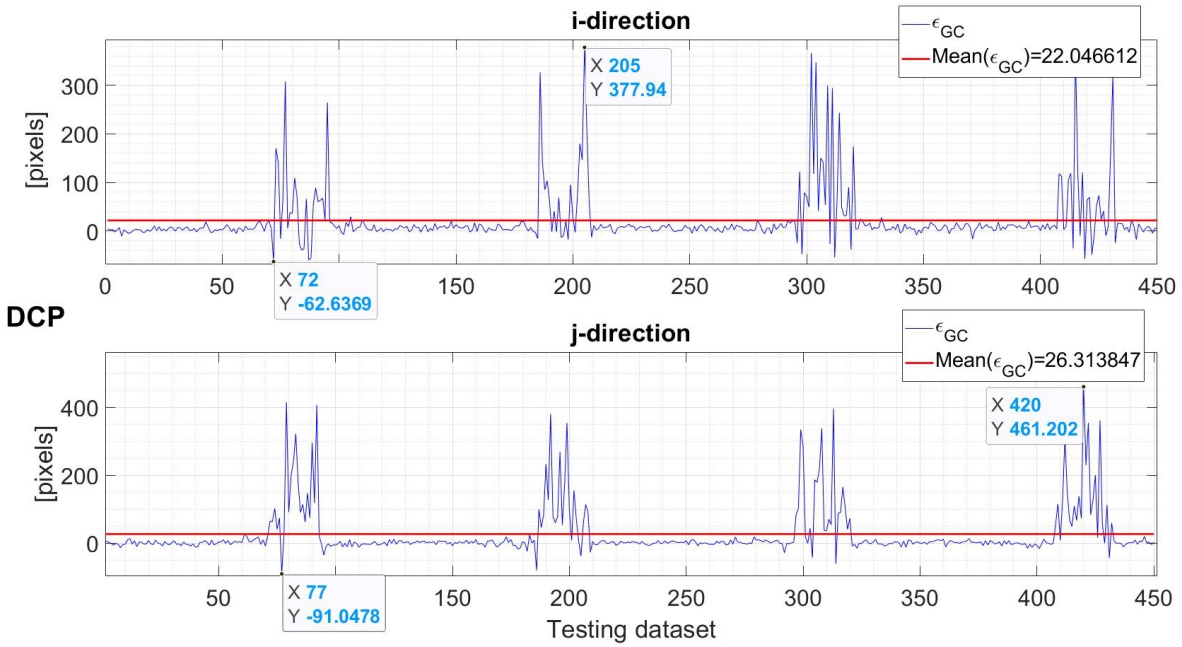

Figure 9: ε_{GC} for DCP

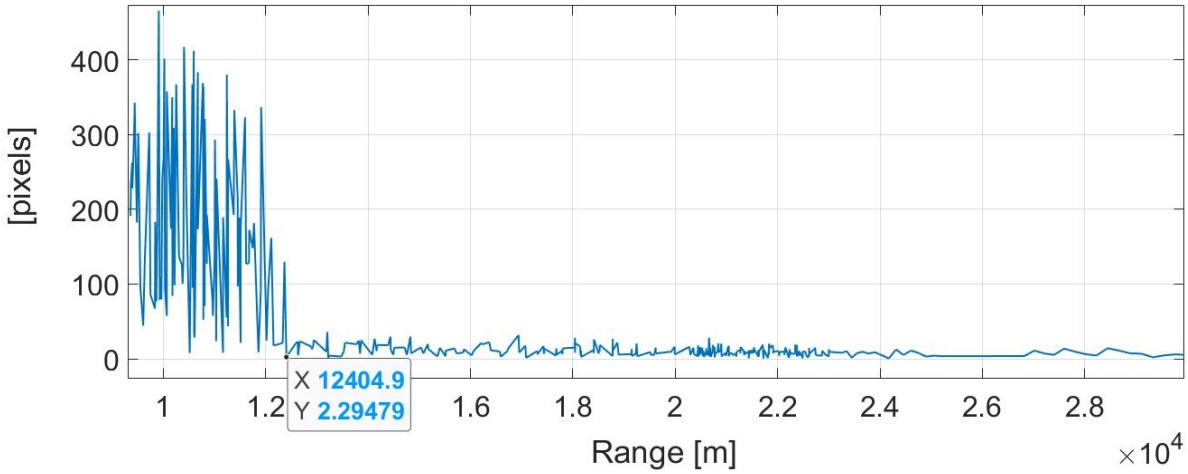

Figure 10: Error between the estimated pixel position of GC and the GT vs range of DCP

and $RMSE_j = 6.01$ pixels. The difference of these values from the ones presented in Section 4.1.1 is negligible, hence the performance of the HRNet-based IP algorithm is not affected by the shape of the asteroid being partially outside of the image. Figure 8 shows two examples of the results obtained in these conditions.

4.3. DCP

4.3.1. Accuracy

Figure 9 illustrates the centroiding results of Didymos for the i- and j-directions of the PANGU viewer for the 450 images of the testing dataset of the DCP. The average value of the error is 22.04 pixels for the i-direction and 26.31 pixels for the j-direction. The RMSE values of this centroiding algorithm are $RMSE_i = 62.03$ pixels and $RMSE_j =$

79.22 pixels, respectively. Since during DCP the range to the asteroid is smaller, the asteroid appears bigger in size in the images and the estimation accuracy is lower than that of the ECP. This is also illustrated by comparing Figure 9 with Figure 4. The epochs when the spacecraft is getting closer to Didymos coincides with the increase of the error of the estimation of the centroid.
Figure 10 shows the norm of the DCP ε_{GC} error of both directions for each image with respect to the range. It can be seen that when the range value is larger than $12,404.9\ m$, the asteroid is far enough for the HRNet-based IP algorithm to provide high accuracy estimation of the centroid. The number of images that represents the asteroid with a range lower than $12,404.9\ m$ is 102. Therefore, the HRNet-based IP algorithm provides accurate results for 77.33% of the DCP images.

5. Conclusion

This paper develops a CNN-based IP algorithm solving the centroiding problem of a binary asteroid system. The ECP and DCP proximity operations of HERA mission to Didymos system are studied as case scenario. The main objective of the developed methodology is to tackle the challenges represented by adverse illumination conditions of the target and by the shape of the target not fully included in the image. The database of images is generated using the software PANGU. The chosen CNN architecture is the HRNet, being the state of the art in keypoint detection, and being already exploited for spaceborn applications. The training and validation datasets are generated with the ECP while the testing dataset with the ECP and the DCP.
The results show that the HRNet-based IP algorithm is able to estimate the centroid of the primary with high accuracy during the ECP regardless of the Sun phase angle. In particular the method is robust to images that are not displaying totally the asteroid. For the DCP the algorithm can provide an accurate estimation of the centroid of the asteroid if the range is larger than a threshold value of $12,404.9\ m$. Considering that the minimum range used for the training was $20,000\ m$, the HRNet-based IP algorithm is able to generalize the estimation for the extra $7596\ m$. If higher accuracy is required for lower ranges, the training database can be augmented using additional images generated with the DCP.
Future work would go into the direction of other utilizations for the HRNet-based IP algorithm. For instance, additional estimated outputs that are useful for the navigation algorithm of the GNC system during the proximity operations with the asteroid are the range from Didymos and the Sun phase angle.

Acknowledgments

This study is co-funded and supported by the European Space Agency under the Open Space Innovation Platform and supported by the GMV Defence and Space . The authors would like to thank Florin-Adrian Stancu for providing the model of Didymos in PANGU, and Marcos Avilés Rodrigálvarez for providing the DCP trajectory data. The authors would also like to acknowledge the support of the entire Aerospace Centre of Excellence of University of Strathclyde.

References

[1] P. Michel, A. F. Cheng, M. Küppers, Asteroid Impact and Deflection Assessment (AIDA) mission: science investigation of a binary system and mitigation test, in: European Planetary Science Congress, Nantes, France, pp. 123–124. October, 2015.

[2] P. Michel, M. Küppers, I. Carnelli, The Hera mission: European component of the ESA-NASA AIDA mission to a binary asteroid, in: COSPAR Scientific Assembly. 2018.

[3] HERA Didymos reference model, ESA Headquarters, 2021.

[4] HERA: Proximity Operations Guidelines, ESA Estec, 2020.

[5] A. Pellacani, M. Graziano, M. Fittock, J. Gil, I. Carnelli, HERA vision based GNC and autonomy, in: European Conference for AeroSpace Sciences, pp. 1–14.

[6] J. Gíl-Fernandez, G. Ortega-Hernando, Autonomous vision-based navigation for proximity operations around binary asteroids, CEAS Space Journal 10 (2018) 287–204.

[7] M. Pugliatti, V. Franzese, F. Topputo, Data-Driven Image Processing for Onboard Optical Navigation Around a Binary Asteroid, Journal of Spacecraft and Rockets (2022) 1–17.

[8] J. A. Christian, E. G. Lightsey, Onboard Image-Processing Algorithm for a Spacecraft Optical Navigation Sensor System, Journal of Spacecraft and Rockets 49 (2012) 337–352.

[9] J. A. Christian, Optical navigation using planet's centroid and apparent diameter in image, Journal of Guidance, Control, and Dynamics 38 (2015) 192–204.

[10] L. P. Cassinis, A. Menicucci, E. Gill, I. Ahrns, J. Gíl-Fernandez, On-Ground Validation of a CNN-based Monocular Pose Estimation System for Uncooperative Spacecraft, in: 8th European Conference on Space Debris. 2021.

[11] K. Sun, B. Xiao, L. Dong, J. Wang, Deep high-resolution representation learning for human pose estimation, in: Proceedings of the IEEE Computer Society Conference on Computer Vision and Pattern Recognition, pp. 5686–5696. June, 2019.

[12] NASA, JPL Solar System Dynamics, 2021.

[13] Planet and Asteroid Natural Scene Generation Utility User Manual, Dundee University, 2019.

[14] ESA, Hera mission instruments, 2021.